



PHOTONICS Research

Multi-gigahertz mode-locked femtosecond Yb:KLuW waveguide lasers

Ji Eun Bae,¹  Xavier Mateos,²  Magdalena Aguiló,² Francesc Díaz,² Javier García Ajates,³ Carolina Romero,³  Javier Rodríguez Vázquez de Aldana,³ and Fabian Rotermund^{1,*}

¹Department of Physics, Korea Advanced Institute of Science and Technology (KAIST), 34141 Daejeon, Republic of Korea

²Universitat Rovira i Virgili (URV), Física i Cristal·lografia de Materials i Nanomaterials (FiCMA), 43007 Tarragona, Spain

³Grupo de Investigación en Aplicaciones del Láser y Fotónica, University of Salamanca, 37008 Salamanca, Spain

*Corresponding author: rotermund@kaist.ac.kr

Received 26 July 2022; revised 6 September 2022; accepted 6 September 2022; posted 12 September 2022 (Doc. ID 471688); published 28 October 2022

We demonstrate multi-gigahertz continuous-wave mode-locking of a Yb:KLuW waveguide laser. A femtosecond-laser-inscribed Yb:KLuW channel waveguide in an extended laser cavity delivers a fundamentally mode-locked laser near 1030 nm. A tunable few-centimeter-long cavity containing a single-walled carbon nanotube saturable absorber as mode-locker generates self-starting femtosecond pulses with average output powers exceeding 210 mW at repetition rates of 2.27, 2.69, and 3.55 GHz. The laser cavity, which includes a wedged waveguide, is extended by using a lens pair that controls the laser fluence on the saturable absorber for reliable mode-locked operation without instability. The presented laser performance, mode-locked up to 3.55 GHz, highly suggests the potential of crystalline Yb:KLuW waveguides for realizing high-power ultrafast lasers with higher GHz repetition rates in a quasi-monolithic cavity. © 2022 Chinese Laser Press

<https://doi.org/10.1364/PRJ.471688>

1. INTRODUCTION

High-repetition-rate ultrafast laser pulses operating at the GHz-level, directly achievable from fundamentally mode-locked compact laser systems, are of great interest in diverse scientific applications, such as astronomy, frequency-comb-based precise metrology, and integrated on-chip photonics [1–5]. Therefore, developing a laser system in an ultra-compact size for practical real-world applications is in high demand. Recently, it was confirmed that waveguides (WGs) inscribed in laser gain media are one of the most promising strategies used to miniaturize solid-state lasers. Tightly confined propagation of the laser beam within the micrometric-volume channel WGs, resulting in high laser efficiency and well-defined single-mode operation, can be obtained by utilizing the femtosecond direct laser writing (fs-DLW) method. The fs-DLW method provides reliable and relatively simple fabrication of flexible three-dimensional structures [6–8]. Recently, GHz mode-locking of WG lasers has been investigated for their own advantages and applications mentioned above [9–16].

As promising WG laser gain media in the 1- μm spectral range, ytterbium ions (Yb^{3+}) have been recognized as attractive dopants for establishing novel laser materials. In particular, Yb^{3+} -doped gain media can be pumped with commercially available laser diodes and typically exhibit broad gain bandwidths and small quantum defects (high Stokes efficiency),

resulting in low thermal loading beneficial for high-power ultrafast lasers. Compared to glass host materials, Yb^{3+} -doped crystals particularly benefit from high absorption and high emission cross-sections, superior thermal properties, and high damage threshold [7,17–20], although laser glasses typically feature a broadband transition that benefits from ultrashort pulse generation. Among the crystalline host materials for Yb^{3+} doping, monoclinic potassium double tungstates, such as $\text{KLu}(\text{WO}_4)_2$ (KLuW), $\text{KY}(\text{WO}_4)_2$ (KYW), and $\text{KGd}(\text{WO}_4)_2$ (KGW), exhibit relatively high and broad emission cross sections, which can bridge the gap between crystals and glasses. High emission cross-sections are also essential for mode-locked operations to avoid Q -switching instabilities. In particular, KLuW exhibits Stark energy level splitting of the ground and excited states because Yb^{3+} doping produces a stronger crystal field compared to KYW and KGW, which is advantageous for ultrashort pulsed laser operation [21–23]. In addition, this crystal can be Yb^{3+} -doped with higher concentrations (up to 100% atomic fraction) without substantial fluorescence quenching while maintaining the monoclinic symmetry and thermal conductivity due to close ionic radii and masses of Yb^{3+} and Lu^{3+} [24]. However, glass hosts show limited doping concentrations for preventing quenching. Consequently, Yb^{3+} -doped monoclinic double tungstates, especially KLuW (Yb:KLuW), are highly attractive host-dopant combinations for efficient high-power ultrafast WG lasers, providing a certain trade-off in

terms of spectroscopic and physical properties given the advantages and limitations.

In recent years, passive mode-locking of WG lasers in the GHz range has been demonstrated utilizing saturable absorbers (SAs), including semiconductor saturable absorber mirrors [9–11,13] and low-dimensional nanomaterials [12,14–16]. Toward high fundamental repetition rate mode-locking in a miniaturized laser cavity, integration flexibility embedded into the cavity is an essential factor. Also, precise controllability of low-level modulation depths with small non-saturable loss is a crucial requirement for preventing Q -switching instabilities, which is much difficult to meet the lower critical pulse energy for higher repetition frequency [25]. Relaxation time should be sufficiently short in order to be recovered within the GHz-cavity round-trip time. One promising SA candidate satisfying the requirements is single-walled carbon nanotubes (SWCNTs). SWCNT-SAs have been recognized as promising SAs that are applicable to diverse WG lasers for various types of interaction with the laser mode through evanescent fields as well as transmissive/reflective fields [14,26–31]. Finely adjustable nonlinear absorption with low non-saturable loss is also possible with relatively simple and cost-effective fabrication processes compared to other two-dimensional nanomaterials [32]. It also provides unique optical properties, including ultra-fast response time and intrinsic ultra-broadband nonlinear absorption.

In this work, to the best of our knowledge, mode-locked Yb:KLuW WG lasers at tunable multi-GHz repetition rates are demonstrated for the first time. The mode-locked pulsed operation by SWCNT-SAs emits a stable train of self-starting femtosecond pulses from a few-centimeter-long cavity. The mode-locking is achievable at a fundamental repetition rate up to 3.55 GHz, with an average output power exceeding 210 mW. The Yb:KLuW WG in an extended cavity, including a lens pair and an SWCNT-SA-coated end mirror, ensures high stability with properly adjusted fluence on the SA. The wedged WG end facet additionally suppresses the residual oscillation within the WG which destabilizes the extended-cavity mode. The continuous-wave (CW) mode-locking is verified, and the laser performance is investigated at repetition rates of 2.27, 2.69, and 3.55 GHz. The multi-GHz mode-locking achieved in this study is the highest oscillation frequency ever reported for a WG laser with an extended cavity. The obtained pulse duration provides the first femtosecond GHz mode-locking achieved at 1 μm in a crystalline WG. The presented laser characteristics indicate the tremendous potential for Yb:KLuW WG to further facilitate femtosecond mode-locking at higher frequencies with up-scaling the output power performance.

2. EXPERIMENTAL METHODS

A. Fabrication of Waveguide and Saturable Absorber

A bulk 5% (atomic fraction) Yb³⁺-doped monoclinic potassium lutetium double tungstate crystal, Yb:KLuW, grown by the top-seeded-solution growth slow-cooling method with K₂W₂O₇ as a solvent [24], is used as the gain medium. One of the uncoated laser-grade polished faces, which are parallel to the N_g axis (length of 3.3 mm and refractive index of 2.03) is wedged by 5°. As mentioned, this wedge contributes to

avoiding etalon effects in the crystal and prevents mode-locking instabilities in the extended cavity scheme. This direction of the optical indicatrix allows access to the higher-gain $E||N_m$ polarization [aperture 13.33 mm (N_m) \times 3.07 mm (N_p)]. The fs-DLW depressed-cladding channel WG is fabricated by using an amplified Ti:sapphire laser system (Spitfire, Spectra Physics). The laser emits 60-fs pulses with a central wavelength of 800 nm at a repetition rate of 5 kHz. The pulse energy is finely controlled externally to the laser system with a set of half-wave plates and a linear polarizer and an additional calibrated density filter. After energy control, the beam was focused by a 40 \times microscope lens (NA = 0.65). A value of ~ 30 nJ pulse energy, estimated after the microscope objective, was chosen to produce damage tracks, and the polarization was kept parallel to the scanning direction. That energy value was slightly above the damage threshold for our experimental condition and ensured no cracking of the sample. The WG was fabricated by scanning the sample at a constant speed of 0.6 mm/s, thus inscribing parallel tracks following the desired tubular structure with a WG diameter of 20 μm (Fig. 1). The distortion of the WGs, due to the refractive index mismatch between air and crystal, is corrected in the model codes.

The SWCNT-SA used to initiate mode-locking in this study is fabricated using arc-discharged SWCNT powder (Meijo Nano Carbon Co., Ltd.) whose broad E₂₂ interband absorption is located in the 1- μm -wavelength region. The powders are dissolved in 1,2-dichlorobenzene (o-DCB) with surfactant. After dispersing the solution by ultrasonication for several hours, it is centrifuged for 30 minutes to purify the dispersed solution by eliminating large bundles of nanotubes or impurities. The SWCNT solution is then mixed at a volume ratio of 1:1 with a separately prepared polymethyl methacrylate (PMMA) (Polymer Source, Inc.) solution (100 mg/mL in o-DCB). The SWCNT/PMMA composite solution is uniformly spin-coated on the highly-reflective (HR) end mirror of the laser cavity and dried in a vacuum oven. Note that the same HR mirror deposited with identical SWCNT-SA is used for all mode-locked operations in this study. The SWCNT-SA provides a modulation depth of about 0.7%, a non-saturable loss of 0.5%, and a saturation fluence of 70 $\mu\text{J}/\text{cm}^2$ with a fast and slow relaxation time of about 200 fs and 2 ps, respectively.

B. Laser Setup for Mode-locking

The experimental laser setup for the mode-locked operation of the Yb:KLuW WG laser is shown in Fig. 1. The pump source is a tapered amplified diode laser (TA pro, Toptica Photonics, Inc.) centered at 982 nm, which can be slightly tuned to

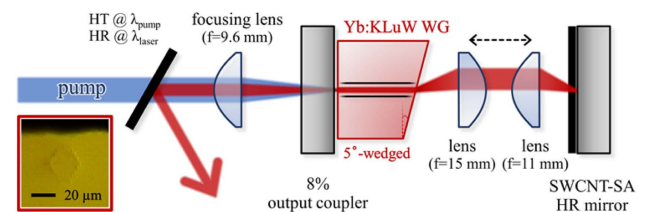


Fig. 1. Schematic of the Yb:KLuW WG laser for SWCNT-SA mode-locking. The optical microscope image (red box) represents the input channel of the fs-DLW Yb:KLuW WG.

maximize the pump absorption of the Yb:KLuW gain medium. The pump beam with a good beam quality of $M^2 < 2.0$ provides a maximum output power of about 2 W just before the cavity. The power and polarization of the pump beam is controlled by a half-wave plate, a polarizer, and another additional half-wave plate. The incident pump polarization is managed to be linearly polarized to $E \parallel N_m$. The pump beam is focused onto the front facet of the Yb:KLuW WG using an aspheric lens ($f = 9.6$ mm) through an 8% output coupler, which is highly transparent (HT) at the pump wavelength. The WG is mounted on a multi-axis stage without any cooling element. To extend the WG laser cavity, a pair of lenses with $f = 15$ mm and $f = 11$ mm is added between the wedged-facet of the WG and the SWCNT-coated HR end mirror. This lens pair can control the laser mode area on the SWCNT-SA to have the sufficient fluence needed for nonlinear absorption and finally stable mode-locking. Note that the SWCNT-coated HR mirror is replaced by a standard HR mirror for CW operation.

3. EXPERIMENTAL RESULTS

Mode-locking results are analyzed in detail for three different repetition frequencies (f_{rep}) up to 3.55 GHz. The repetition rates correspond to the fundamentally mode-locked frequency that is inversely proportional to the optical length of the cavity round trip. The geometrical cavity lengths of the extended WG laser are measured to be 5.8, 4.8, and 3.5 cm for mode-locking at 2.27, 2.69, and 3.55 GHz, respectively. The cavity length can be adjusted by managing the distance between the intra-cavity lens pair (Fig. 1). The mode-locking frequency of 3.55 GHz is the shortest cavity limit achievable by setting the distance between the lens pair to near zero in our cavity.

The mode-locked pulse sequences are recorded with a 12.5-GHz-bandwidth oscilloscope (DPO71254, Tektronix) using a 15-GHz-bandwidth InGaAs photodetector (ET-3500, Electro-Optics Technology, Inc.), as shown in Fig. 2. Figures 2(a), 2(c), and 2(e) show CW mode-locked pulse trains without any unwanted multi-pulsing instabilities or Q-switching signals in a wide time span of 10 μs . The mode-locked states are stably maintained for several days. In a close view with a 7-ns time span, as shown in Figs. 2(b), 2(d), and 2(f), the mode-locked repetitive pulses with a time period of 440, 372, and 281 ps are observed, corresponding to the fundamental mode-locked frequencies of 2.27, 2.69 and 3.55 GHz, respectively.

The stability and reliability of the mode-locked operation are also confirmed by a radio-frequency spectrum analyzer (frequency range of 9 kHz–26.5 GHz, E4407B, Agilent). Figures 3(a), 3(c), and 3(e) show the recorded signals at the fundamental beat notes corresponding to each laser repetition rate and their clear high harmonics measured in a span of 26.5 GHz at a resolution bandwidth (RBW) of 100 kHz. The fundamental mode-locked frequencies are also shown in a frequency span of 2 MHz and an RBW of 1 kHz [Figs. 3(b), 3(d), and 3(f)]. The sharp peaks with a narrow linewidth of ~ 4 kHz at a 3 dB bandwidth ($\Delta f_{-3\text{dB}}$) and a high extinction ratio of over 73 dB indicate a clear evidence for pure and stable mode-locking in all cases. No other instability signals, including Q-switching tendencies, are observed around the mode-locked peaks. Therefore, Fig. 3 further confirms the occurrence

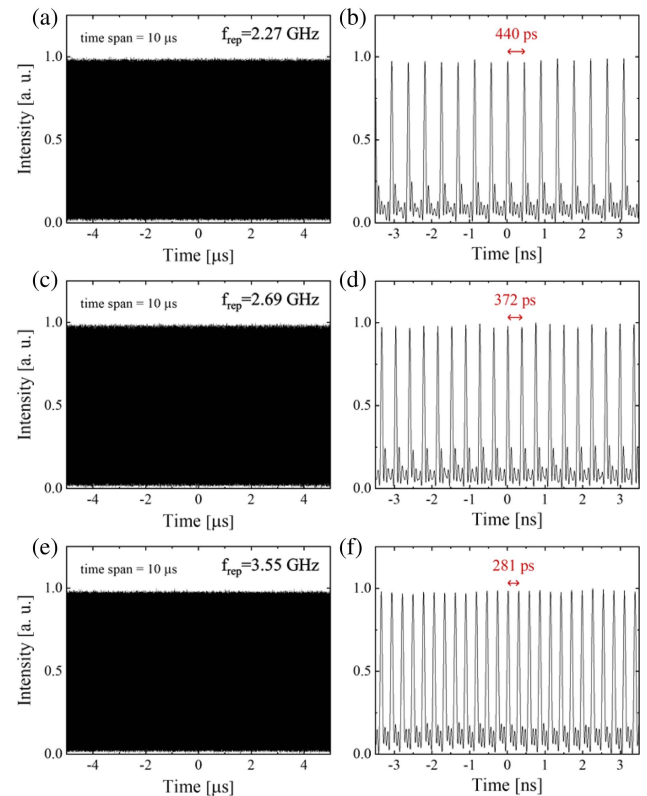


Fig. 2. Oscilloscope traces of the mode-locked pulses at repetition frequencies of (a), (b) 2.27 GHz, (c), (d) 2.69 GHz, and (e), (f) 3.55 GHz in different time spans of 10 μs and 7 ns.

of a highly stable CW mode locking. During the experiment, no degradation in performance is observed, indicating the excellent stability of the SWCNT-SA used. Note that, to the best of our knowledge, the achieved repetition rate of 3.55 GHz is the highest mode-locked frequency for an extended WG laser ever demonstrated up to now.

The mode-locked pulse width at a maximum laser output power is measured with an intensity autocorrelator, as shown in Fig. 4. The autocorrelation traces indicate pulse durations (full-width at half-maximum, FWHM) of 736, 808, and 876 fs, assuming sech^2 pulse shapes at the mode-locked frequencies of 2.27, 2.69, and 3.55 GHz, respectively. The obtained pulse widths represent the first sub-picosecond pulses for any GHz mode-locked crystalline WG lasers in the 1- μm spectral region. The laser spectra are measured by an optical spectrum analyzer (86142A, Agilent) with an RBW of 0.06 nm. The 3.55-GHz mode-locked laser is centered at 1030.6 nm with an FWHM spectral bandwidth of 1.6 nm, as shown in Fig. 5(a). The corresponding time-bandwidth product (TBP) is calculated as 0.396 (the Fourier-transform limit is 0.315), indicating slightly chirped pulses. This is attributed to the absence of precise dispersion compensation in the cavity. The total round-trip cavity group delay dispersion is estimated to be about 1323 fs^2 by taking into account the dispersion of the Yb:KLuW crystal, the lens pair, and the air. Further optimization of dispersion can improve the mode-locked pulse characteristics. For a better comparison, the mode-locked laser performances are summarized in Table 1.

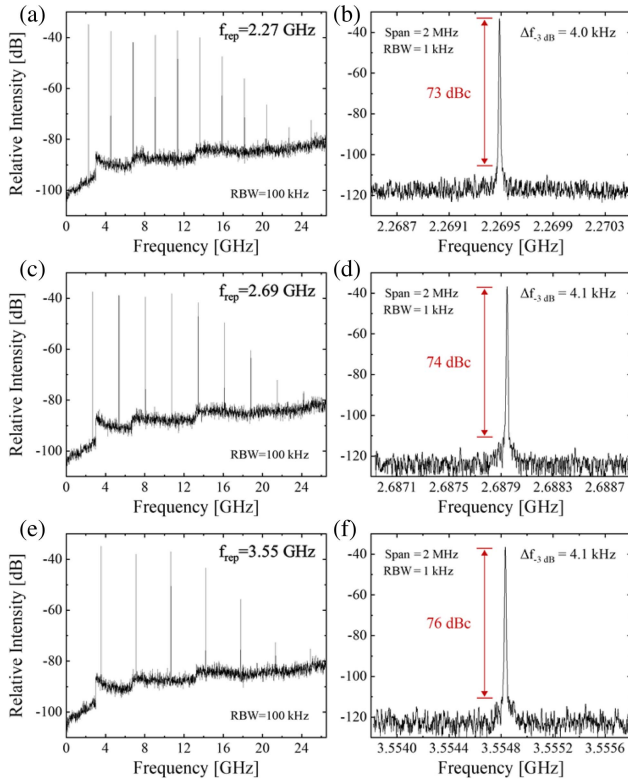


Fig. 3. Radio-frequency spectra of the mode-locked pulses at repetition rates of (a), (b) 2.27 GHz, (c), (d) 2.69 GHz, and (e), (f) 3.55 GHz. (a), (c), and (e) show the harmonics of the mode-locked frequency in a wide frequency span, while (b), (d), and (f) show the fundamental beat note in a 2-MHz-frequency span.

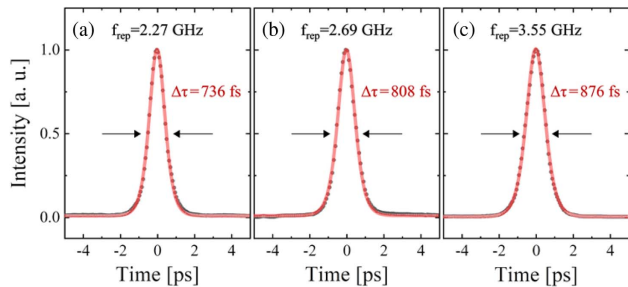


Fig. 4. Autocorrelation traces and their sech^2 fit (red curves) of the mode-locked pulses at repetition rates of (a) 2.27 GHz, (b) 2.69 GHz, and (c) 3.55 GHz at the maximum power.

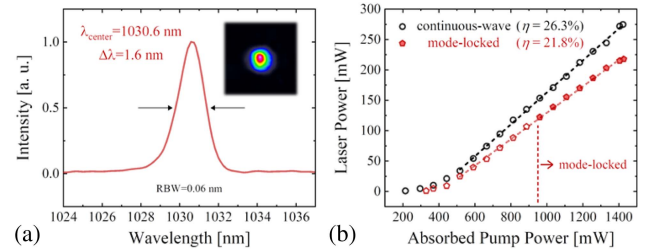


Fig. 5. (a) 3.55-GHz mode-locked laser spectrum (inset: laser beam profile) at the maximum power and (b) average output powers versus absorbed pump powers for the CW and the 3.55-GHz mode-locked operation.

The laser spectra are centered near 1030 nm for all operation modes. The far-field laser mode profiles represent well-defined fundamental modes, as shown in the inset of Fig. 5(a). For the 3.55-GHz mode-locking, Fig. 5(b) shows the laser output powers depending on the absorbed pump power both in the CW operation without the SWCNT-SA and the mode-locked operation employing the SWCNT-SA. The absorbed pump power is estimated from the incident pump power by considering the Fresnel transmission at the WG input facet and the absorption amount under the lasing condition. The slope efficiency for the CW and mode-locked operation is 26.3% and 21.8%, respectively. The maximum mode-locked laser power amounts to 217 mW at an absorbed pump power of 1429 mW. Pulse energy and peak power at the maximum power amount to 61.2 pJ and 69.9 W, respectively. The 3.55-GHz mode-locked operation is self-starting above the absorbed pump power of 953 mW, as shown in Fig. 5(b). At the pump power level between the mode-locking threshold of 953 mW and the lasing threshold of 330 mW, the laser operates in CW or Q-switched mode.

All three operation modes at different repetition rates presented in this work generate higher output powers of >210 mW and slope efficiencies of >20% (Table 1) compared to other GHz mode-locked WG lasers. Note that the output power performance can be slightly lower than that of a typical quasi-monolithic Yb:KLuW cavity configuration with a plane-parallel WG. This is mainly attributed to higher losses at the 5-degree-wedged WG end facet. The internal loss of the cavity is estimated from a modified Caird analysis for the CW mode with an output coupling transmission from 1% to 30% [33]. The resulting loss amounts to ~ 0.62 dB ($\sim 13\%$) per single pass of the cavity. This includes the propagation loss within the WG and the additional losses through the incoupling loss

Table 1. Laser Performance at Three Different Mode-Locking Frequencies (f_{rep})^{a,b}

f_{rep} [GHz]	$P_{CW, \text{max}}$ (η_{CW})	$P_{\text{mode-lock, max}}$ ($\eta_{\text{mode-lock}}$)	$\Delta\lambda$ (λ_{center}) [nm]	$\Delta\tau$ [fs]	TBP
2.27	249 mW (23.4%)	227 mW (22.0%)	2.0 (1030.8)	736	0.415
2.69	272 mW (24.5%)	214 mW (20.4%)	1.7 (1030.8)	808	0.388
3.55	274 mW (26.3%)	217 mW (21.8%)	1.6 (1030.6)	876	0.396

^a $P_{CW, \text{max}}$ (η_{CW}) and $P_{\text{mode-lock, max}}$ ($\eta_{\text{mode-lock}}$) are the maximum laser output power (slope efficiency) for CW and mode-locked operation.

^b $\Delta\lambda$ (λ_{center}) and $\Delta\tau$ denote the FWHM spectral bandwidth (center wavelength) and pulse width of the mode-locked laser at the maximum power.

at the wedged interface of the WG and the intracavity lens pair loss.

4. CONCLUSION

We report the first GHz mode-locked operation of a double-tungstate WG used as a gain medium. The fs-DLW Yb:KLuW WG laser with only a few-centimeter-long cavity, including an SWCNT-SA, is demonstrated to achieve stably mode-locked pulses at multi-GHz repetition rates of 2.27, 2.69, and 3.55 GHz. Self-starting CW mode-locking delivers femtosecond pulses near 1030 nm. The resulting pulse width provides the first sub-picosecond pulse for a GHz mode-locked crystalline WG laser in the 1- μ m spectral range. To the best of our knowledge, the multi-GHz mode-locking result represents the highest mode-locked frequency ever demonstrated with other WG lasers in an extended cavity. The laser operation performance reveals that the Yb:KLuW WG is a promising medium capable of femtosecond-GHz mode-locking with an improved cavity dispersion management. Further development of mode-locking at the GHz level should also be possible with direct integration of an SA on the WG.

Funding. National Research Foundation of Korea (2018H1A2A1061480, 2019R1A2C3003504, 2020R1A4A2002828); MCIN/Agencia Estatal de Investigación (PID2019-108543RB-I00, PID2020-119818GB-I00); Junta de Castilla y León (SA136P20).

Acknowledgment. Xavier Mateos is a Serra Hünter Fellow with the Serra Hünter Programme, Catalan University, Spain.

Disclosures. The authors declare no conflicts of interest.

Data Availability. Data underlying the results presented in this paper are not publicly available at this time but may be obtained from the authors upon reasonable request.

REFERENCES

1. T. M. Fortier, A. Bartels, and S. A. Diddams, "Octave-spanning Ti:sapphire laser with a repetition rate >1 GHz for optical frequency measurements and comparisons," *Opt. Lett.* **31**, 1011–1013 (2006).
2. M. P. Moreno and S. S. Vianna, "Femtosecond 1 GHz Ti:sapphire laser as a tool for coherent spectroscopy in atomic vapor," *J. Opt. Soc. Am. B* **28**, 2066–2069 (2011).
3. S. Pekarek, T. Südmeyer, S. Lecomte, S. Kundermann, J. M. Dudley, and U. Keller, "Self-referenceable frequency comb from a gigahertz diode-pumped solid-state laser," *Opt. Express* **19**, 16491–16497 (2011).
4. C. Kerse, H. Kalaycioglu, P. Elahi, B. Çetin, D. K. Kesim, O. Akçaalan, S. Yavas, M. D. Asik, B. Öktem, H. Hoogland, R. Holzwarth, and F. Ö. Ilday, "Ablation-cooled material removal with ultrafast bursts of pulses," *Nature* **537**, 84–88 (2016).
5. R. A. McCracken, J. M. Charsley, and D. T. Reid, "A decade of astrocombs: recent advances in frequency combs for astronomy [Invited]," *Opt. Express* **25**, 15058–15078 (2017).
6. F. Chen and J. R. V. de Aldana, "Optical waveguides in crystalline dielectric materials produced by femtosecond-laser micromachining," *Laser Photon. Rev.* **8**, 251–275 (2014).
7. T. Calmano and S. Müller, "Crystalline waveguide lasers in the visible and near-infrared spectral range," *IEEE J. Sel. Top. Quantum Electron.* **21**, 401–413 (2015).
8. J. E. Bae, T. Calmano, C. Kränkel, and F. Rotermund, "Controllable dynamic single- and dual-channel graphene Q-switching in a beam-splitter-type channel waveguide laser," *Laser Photon. Rev.* **16**, 2100501 (2022).
9. A. Choudhary, A. A. Lagatsky, P. Kannan, W. Sibbett, C. T. A. Brown, and D. P. Shepherd, "Diode-pumped femtosecond solid-state waveguide laser with a 4.9 GHz pulse repetition rate," *Opt. Lett.* **37**, 4416–4418 (2012).
10. A. A. Lagatsky, A. Choudhary, P. Kannan, D. P. Shepherd, W. Sibbett, and C. T. A. Brown, "Fundamentally mode-locked, femtosecond waveguide oscillators with multi-gigahertz repetition frequencies up to 15 GHz," *Opt. Express* **21**, 19608–19614 (2013).
11. A. Choudhary, A. A. Lagatsky, Z. Y. Zhang, K. J. Zhou, Q. Wang, R. A. Hogg, K. Pradeesh, E. U. Rafailov, W. Sibbett, C. T. A. Brown, and D. P. Shepherd, "A diode-pumped 1.5 μ m waveguide laser mode-locked at 6.8 GHz by a quantum dot SESAM," *Laser Phys. Lett.* **10**, 105803 (2013).
12. A. G. Okhrimchuk and P. A. Obratsov, "11-GHz waveguide Nd:YAG laser CW mode-locked with single-layer graphene," *Sci. Rep.* **5**, 11172 (2015).
13. C. Khurmi, N. B. Hébert, W. Q. Zhang, S. Afshar, G. Chen, J. Genest, T. M. Monro, and D. G. Lancaster, "Ultrafast pulse generation in a mode-locked erbium chip waveguide laser," *Opt. Express* **24**, 27177–27183 (2016).
14. S. Y. Choi, T. Calmano, F. Rotermund, and C. Kränkel, "2-GHz carbon nanotube mode-locked Yb:YAG channel waveguide laser," *Opt. Express* **26**, 5140–5145 (2018).
15. Z. Li, N. Dong, Y. Zhang, J. Wang, H. Yu, and F. Chen, "Invited Article: Mode-locked waveguide lasers modulated by rhenium diselenide as a new saturable absorber," *APL Photon.* **3**, 080802 (2018).
16. C. Grivas, R. Ismaeel, C. Corbari, C.-C. Huang, D. W. Hewak, P. Lagoudakis, and G. Brambilla, "Generation of multi-gigahertz trains of phase-coherent femtosecond laser pulses in Ti:sapphire waveguides," *Laser Photon. Rev.* **12**, 1800167 (2018).
17. R. Peters, C. Kränkel, K. Petermann, and G. Huber, "Broadly tunable high-power Yb:Lu₂O₃ thin disk laser with 80% slope efficiency," *Opt. Express* **15**, 7075–7082 (2007).
18. J. Liu, V. Petrov, X. Mateos, H. Zhang, and J. Wang, "Efficient high-power laser operation of Yb:KLu(WO₄)₂ crystals cut along the principal optical axes," *Opt. Lett.* **32**, 2016–2018 (2007).
19. T. Calmano, J. Siebenmorgen, A.-G. Paschke, C. Fiebig, K. Paschke, G. Erbert, K. Petermann, and G. Huber, "Diode pumped high power operation of a femtosecond laser inscribed Yb:YAG waveguide laser [Invited]," *Opt. Mater. Express* **1**, 428–433 (2011).
20. F. Druon, S. Ricaud, D. N. Papadopoulos, A. Pellegrina, P. Camy, J. L. Doualan, R. Moncorgé, A. Courjaud, E. Mottay, and P. Georges, "On Yb:CaF₂ and Yb:SrF₂: review of spectroscopic and thermal properties and their impact on femtosecond and high power laser performance [Invited]," *Opt. Mater. Express* **1**, 489–502 (2011).
21. A. Schmidt, S. Rivier, G. Steinmeyer, J. H. Yim, W. B. Cho, S. Lee, F. Rotermund, M. C. Pujol, X. Mateos, M. Aguiló, F. Díaz, V. Petrov, and U. Griebner, "Passive mode locking of Yb:KLuW using a single-walled carbon nanotube saturable absorber," *Opt. Lett.* **33**, 729–731 (2008).
22. E. Ugolotti, A. Schmidt, V. Petrov, J. W. Kim, D.-I. Yeom, F. Rotermund, S. Bae, B. H. Hong, A. Agnesi, C. Fiebig, G. Erbert, X. Mateos, M. Aguiló, F. Díaz, and U. Griebner, "Graphene mode-locked femtosecond Yb:KLuW laser," *Appl. Phys. Lett.* **101**, 161112 (2012).
23. S. Y. Choi, J. W. Kim, M. H. Kim, D.-I. Yeom, B. H. Hong, X. Mateos, M. Aguiló, F. Díaz, V. Petrov, U. Griebner, and F. Rotermund, "Carbon nanostructure-based saturable absorber mirror for a diode-pumped 500-MHz femtosecond Yb:KLu(WO₄)₂ laser," *Opt. Express* **22**, 15626–15631 (2014).
24. V. Petrov, M. C. Pujol, X. Mateos, Ò. Silvestre, S. Rivier, M. Aguiló, R. M. Solé, J. H. Liu, U. Griebner, and F. Díaz, "Growth and properties of KLu(WO₄)₂ and novel ytterbium and thulium lasers based on this monoclinic crystalline host," *Laser Photon. Rev.* **1**, 179–212 (2007).
25. C. Hönninger, R. Paschotta, F. Morier-Genoud, M. Moser, and U. Keller, "Q-switching stability limits of continuous-wave passive mode locking," *J. Opt. Soc. Am. B* **16**, 46–56 (1999).

26. S. J. Beecher, R. R. Thomson, N. D. Psaila, Z. Sun, T. Hasan, A. G. Rozhin, A. C. Ferrari, and A. K. Kar, "320 fs pulse generation from an ultrafast laser inscribed waveguide laser mode-locked by a nanotube saturable absorber," *Appl. Phys. Lett.* **97**, 111114 (2010).
27. E. Kifle, X. Mateos, P. Loiko, S. Y. Choi, J. E. Bae, F. Rotermund, M. Aguiló, F. Díaz, U. Griebner, and V. Petrov, "Tm:KY_{1-x-y}Gd_xLu_y(WO₄)₂ planar waveguide laser passively Q-switched by single-walled carbon nanotubes," *Opt. Express* **26**, 4961–4966 (2018).
28. E. Kifle, P. Loiko, J. R. V. de Aldana, C. Romero, A. Ródenas, S. Y. Choi, J. E. Bae, F. Rotermund, V. Zakharov, A. Veniaminov, M. Aguiló, F. Díaz, U. Griebner, V. Petrov, and X. Mateos, "Passively Q-switched femtosecond-laser-written thulium waveguide laser based on evanescent field interaction with carbon nanotubes," *Photon. Res.* **6**, 971–980 (2018).
29. J. W. Kim, S. Y. Choi, J. E. Bae, M. H. Kim, Y. U. Jeong, E. Kifle, X. Mateos, M. Aguiló, F. Díaz, U. Griebner, V. Petrov, G.-H. Kim, and F. Rotermund, "Comparative study of Yb:KYW planar waveguide lasers Q-switched by direct- and evanescent-field interaction with carbon nanotubes," *Opt. Express* **27**, 1488–1496 (2019).
30. J. E. Bae, T. G. Park, E. Kifle, X. Mateos, M. Aguiló, F. Díaz, C. Romero, J. R. V. de Aldana, H. Lee, and F. Rotermund, "Carbon nanotube Q-switched Yb:KLuW surface channel waveguide lasers," *Opt. Lett.* **45**, 216–219 (2020).
31. J. E. Bae, S. Y. Choi, C. Kränkel, K. Hasse, and F. Rotermund, "Evanescent-field Q-switched Yb:YAG channel waveguide lasers with single- and double-pass pumping," *Curr. Opt. Photon.* **5**, 180–185 (2021).
32. J. E. Bae, X. Mateos, M. Aguiló, F. Díaz, J. R. V. de Aldana, C. Romero, H. Lee, and F. Rotermund, "Transition of pulsed operation from Q-switching to continuous-wave mode-locking in a Yb:KLuW waveguide laser," *Opt. Express* **28**, 18027–18034 (2020).
33. J. A. Caird, S. A. Payne, P. R. Staber, A. J. Ramponi, L. L. Chase, and W. F. Krupke, "Quantum electronic properties of the Na₃Ga₂Li₃F₁₂:Cr³⁺ Laser," *IEEE J. Quantum Electron.* **24**, 1077–1099 (1988).